Relative Dymamic Stability of a One-machine System : Frequency-response Approach

AUTHOR(S):

OHSAWA, Yasuharu; HAYASHI, Muneaki

CITATION:

OHSAWA, Yasuharu ...[et al]. Relative Dymamic Stability of a One-machine System : Frequency-response Approach. Memoirs of the Faculty of Engineering, Kyoto University 1972, 33(4): 307-328

ISSUE DATE:

1972-03-31

URL:

http://hdl.handle.net/2433/280863

Relative Dymamic Stability of a One-machine System

—Frequency-response Approach—

By

Yasuharu OHSAWA* and Muneaki HAYASHI*

(Received June 30, 1971)

A one-machine system under small perturbations was represented in a closed-loop block diagram and its open-loop transfer function was calculated. The concept of relative stability was developed by means of a generalized Nyquist's criterion. Moreover, the indicial response of terminal voltage according to the unit step change of excitation voltage was calculated by means of a Fourier series approximation and its integral squared error was proposed as a measure of relative stability. A stability analysis using this measure was developed for various values of power output. Also, the effects of the regulator gain were analyzed using this measure.

1. Introduction

The stability problem of a synchronous machine has received a great deal of attention in the past[1,2,3] and will receive increasing attention in the future, since it is to be expected that leading power-factor operation of synchronous generators under lightly loaded conditions will become difficult to avoid and generation and transmission equipment will come to be applied with higher reactances and correspondingly lower stability margins. Among several aspects of the stability of a synchronous machine, an important one is the mode of small perturbation stability. This paper deals with an analysis of the phenomena of stability of synchronous machines under small perturbations by examining the case of a single machine connected to a large system through an external impedance.

First described is a method of representing the perturbed performance of a one-machine system in the closed-loop block diagram. A detailed model of a synchronous machine equipped with damper windings and the effects of excitation and prime mover controls are included, in order to make the analysis more accurate.

* Institute of Electrical Engineering

A knowledge of the degree of stability is frequently more important than merely knowing whether, under certain operating conditions, the machine is stable or not. A concept of relative stability was developed by means of a generalized Nyquist's criterion.

Moreover, the variation of terminal voltage responding to the step change of excitation voltage was calculated by means of a Fourier series approximation and its integral squared error was examined as a measure of relative stability. The stability analysis using this measure was developed for various values of power output. Also, the effects of the regulator gain were analyzed using this measure.

2. Representation of Systems for Stability Analysis

2-1 Description of a Synchronous Machine

Complete description of the dynamic behavior of a synchronous machine requires consideration of its electrical and mechanical characteristics as well as those of associated control systems. The necessary mathematical statements are summarized here.

The equations describing the balanced 3-phase performance of a synchronous machine were derived by the use of Park's axis transformation shown in several references (Appendix A) and summarized by Shackshaft[1]. They are subject to the following assumptions:

(a) A current in any winding is assumed to set up an m. m. f. wave which is sinusoidally distributed in space around the air gap.

(b) The effects of hysteresis are neglected.

(c) It was assumed that a component of m. m. f. acting along the direct axis produces a sinusoidally distributed flux wave in that axis only, and that, similarly, a quadrature-axis m. m. f. produces only a quadrature-axis flux.

The equations are shown in Appendix B. Time is scaled so as to make ω_0 unity: i. e., real time was multiplied by $2\pi f_0$ in this paper. The equations are represented in per-unit form. The base values chosen were such that all per-unit mutual inductances between rotor and stator circuits in each axis were equal to one another. On this basis the following relations between self-, mutual, and leakage reactances pertain:[2]

$$\begin{aligned} x_{ffd} &= x_{ad} + x_{fl} & x_q &= x_{aq} + x_{al} \\ x_d &= x_{ad} + x_{al} & x_{kkq} &= x_{aq} + x_{kql} \\ x_{kkd} &= x_{ad} + x_{kdl} \end{aligned} \tag{1}$$

The nomenclature is summarized at the conclusion of the paper.

If ψ_{fd}, ψ_{kd}, i_{fd}, and i_{kd} are eliminated from eqns. (B-1)-(B-3), (B-6), and (B-8), the expression for ψ_d becomes

$$\psi_d=\frac{\{(x_{kkd}-x_{fkd})s+r_{kd}\}x_{ad}}{(x_{ffd}\cdot x_{kkd}-x_{fkd}^2)s^2+(r_{fd}\cdot x_{kkd}+r_{kd}\cdot x_{ffd})s+r_{fd}\cdot r_{kd}}v_{fd}$$
$$-\left[x_d-\frac{\{(x_{kkd}+x_{ffd}-2x_{fkd})s^2+(r_{kd}+r_{fd})s\}x_{ad}^2}{(x_{ffd}\cdot x_{kkd}-x_{fkd}^2)s^2+(r_{fd}\cdot x_{kkd}+r_{kd}\cdot x_{ffd})s+r_{fd}\cdot r_{kd}}\right]i_d \tag{2}$$

Eqn. (2) is rewritten as follows:

$$\psi_d=G(s)\cdot v_{fd}-X_d(s)\cdot i_d \tag{3}$$

Similarly, eliminating ψ_{kq} and i_{kq} from eqns. (B-4), (B-5), and (B-10) yields

$$\psi_q=-\left(x_q-\frac{x_{aq}^2 s}{x_{kkq}s+r_{kq}}\right)i_q \tag{4}$$

and

$$\psi_q=-X_q(s)i_q \tag{5}$$

The quantities $X_d(s)$ and $X_q(s)$ are called operational reactances and $G(s)$ is called an operational transfer function.

The equations describing a one-machine system shown in Figs. 1 and 2 are as follows:

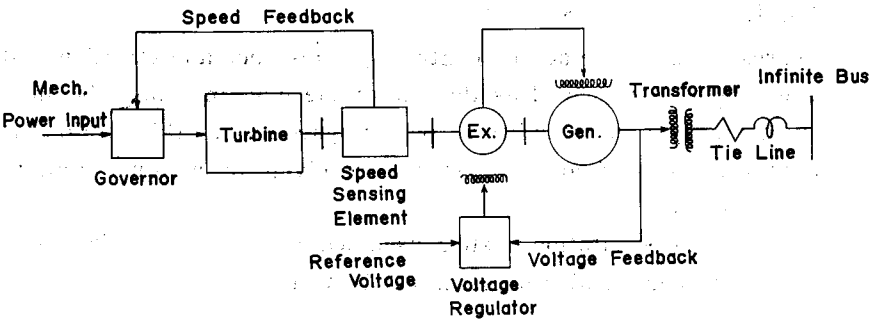

Fig. 1. Model system (1).

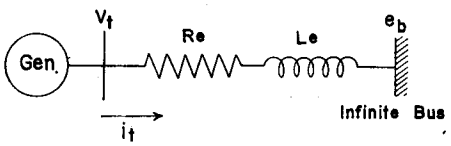

Fig. 2. Model system (2).

Stator flux linkages

$$\psi_d=G(s)\cdot v_{fd}-X_d(s)\cdot i_d \tag{6}$$

$$\psi_q=-X_q(s)\cdot i_q \tag{7}$$

Induced voltages

$$v_d = s\psi_d - r \cdot i_d - \omega\psi_q \tag{8}$$

$$v_q = s\psi_q - r \cdot i_q + \omega\psi_d \tag{9}$$

Voltages at the infinite bus

$$e_d = s(\psi_d - L_e \cdot i_d) - (r + R_e) \cdot i_d - \omega \cdot (\psi_q - L_e \cdot i_q) \tag{10}$$

$$e_q = s(\psi_q - L_e \cdot i_q) - (r + R_e) \cdot i_q + \omega \cdot (\psi_d - L_e \cdot i_d) \tag{11}$$

$$e_d = e_b \sin\delta \tag{12}$$

$$e_q = e_b \cos\delta \tag{13}$$

Electrical torque at air gap

$$T = \psi_d \cdot i_q - \psi_q \cdot i_d \tag{14}$$

Terminal voltage

$$v_t^2 = v_d^2 + v_q^2 \tag{15}$$

Mechanical equation

$$Ms\omega = T_M - T \tag{16}$$

Angular relation

$$s\delta = \omega \tag{17}$$

2-2 Description of Control Systems

The representation of machine control systems such as excitation systems and the speed governor as well as the one of the machine must be included in a study of the dynamic stability of power systems. In this section mathematical representations of control systems are given in a form appropriate for stability studies.

The model of the excitation system assumed in this paper is shown in Fig. 3, and its mathematical representation is as follows:

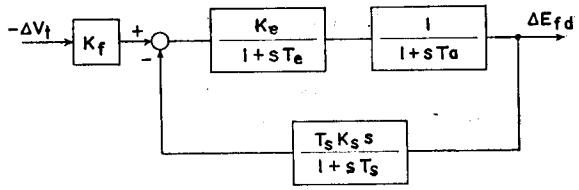

Fig. 3. Simplified model of voltage regulator.

$$g(s) = \frac{K_e \cdot K_r (1 + T_s s)}{(1 + T_e s)(1 + T_s s)(1 + T_a s) + K_e K_s s} \tag{18}$$

The saturation of amplifiers, non-linearity of rectifiers, and time-lags between the movements of elements or equipment are neglected to simplify the calculation. The values of the gain K_r are varied later.

Under restrictions similar to the ones of AVR, a simplified model of the speed governor is shown in Fig. 4 and represented as follows:

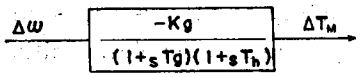

Fig. 4. Simplified model of governor.

$$M(s)=\frac{K_g}{(1+T_g s)(1+T_h s)} \tag{19}$$

2-3 Linearized Equations for a One-machine System

When steady-state stability is studied, the complexity can be reduced by considering only small deviations of the variables from their steady-state values. This means that system equations can be linearized, since only infinitesimally small changes are of interest. This method of small oscillation is well known and used in many dynamic stability studies.

Eqns. (6)-(17) are linearized to give:

$$\Delta\psi_d=G(s)\cdot\Delta v_{fd}-X_d(s)\cdot\Delta i_d \tag{20}$$

$$\Delta\psi_q=-X_q(s)\cdot\Delta i_q \tag{21}$$

$$\Delta v_d=-\psi_{q0}\cdot\Delta\omega-\Delta\psi_q-r\cdot\Delta i_d+s\Delta\psi_d \tag{22}$$

$$\Delta v_q=\psi_{d0}\cdot\Delta\omega+\Delta\psi_d-r\cdot\Delta i_q+s\Delta\psi_q \tag{23}$$

$$\Delta e_d=-(\psi_{q0}-i_{q0}\cdot L_e)\cdot\Delta\omega-(\Delta\psi_q-L_e\cdot\Delta i_q)-(R_e+r)\cdot\Delta i_d +s(\Delta\psi_d-L_e\cdot\Delta i_d) \tag{24}$$

$$\Delta e_q=-(\psi_{d0}-i_{d0}\cdot L_e)\cdot\Delta\omega+(\Delta\psi_d-L_e\cdot\Delta i_d)-(R_e+r)\cdot\Delta i_q +s(\Delta\psi_d-L_e\cdot\Delta i_d) \tag{25}$$

$$\Delta e_d=e_{b0}\cos\delta_0\cdot\Delta\delta=e_{q0}\cdot\Delta\delta \tag{26}$$

$$\Delta e_q=-e_{b0}\cdot\sin\delta_0\cdot\Delta\delta=-e_{d0}\cdot\Delta\delta \tag{27}$$

$$\Delta v_t=\frac{v_{d0}}{v_{t0}}\cdot\Delta v_d+\frac{v_{q0}}{v_{t0}}\cdot\Delta v_q \tag{28}$$

$$\Delta T=\psi_{d0}\cdot\Delta i_q+i_{q0}\cdot\Delta\psi_d-\psi_{q0}\cdot\Delta i_d-i_{d0}\cdot\Delta\psi_q \tag{29}$$

$$Ms\Delta\omega=\Delta T_M-\Delta T \tag{30}$$

$$s\Delta\delta=\Delta\omega \tag{31}$$

Voltage regulator

$$\Delta E_{fd}=-g(s)\cdot\Delta v_t \tag{32}$$

$$\Delta v_{fd}=\frac{r_{fd}}{x_{ad}}\cdot\Delta E_{fd} \tag{33}$$

Speed governor

$$\Delta T_M = -M(s) \cdot \Delta\omega \tag{34}$$

2-4 Initial Conditions

Before the dynamic stability of the system is studied, it is necessary to find the initial values of pertinent variables. Initial conditions are obtained by knowing the power output, power factor, terminal voltage, and current. Under steady-state conditions, i_{kd}, i_{kq}, and all the derivative terms are zero.

The situation is represented in the phasor diagram shown in Fig. 5, from which the load angle δ results as

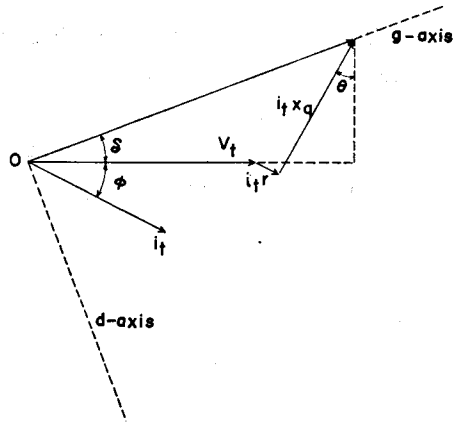

Fig. 5. Phasor diagram for computation of initial load angle.

$$\delta = Imag \cdot [\log\{v_t + i_t \cdot (r + jx_q)\}] \tag{35}$$

Once the load angle δ is determined, other variables may be computed from[2]

$$v_d = v_t \cdot \sin\delta \tag{36}$$

$$v_q = v_t \cdot \cos\delta \tag{37}$$

$$i_d = i_t \cdot \sin(\delta + \phi) \tag{38}$$

$$i_q = i_t \cdot \cos(\delta + \phi) \tag{39}$$

$$\psi_d = v_q + r \cdot i_q \tag{40}$$

$$\psi_q = -v_d - r \cdot i_d \tag{41}$$

The voltage of the infinite bus is therefore set after the initial conditions are obtained.

2-5 Derivation of Transfer Functions

Manipulating eqns. (20)-(34) to obtain a form suitable for closed loop stability analysis, Fig. 6 is obtained[3] (the detailed derivation is shown in Appendix C). This block diagram illustrates the closed loop structure of the equations which include representations of prime-mover power and excitation

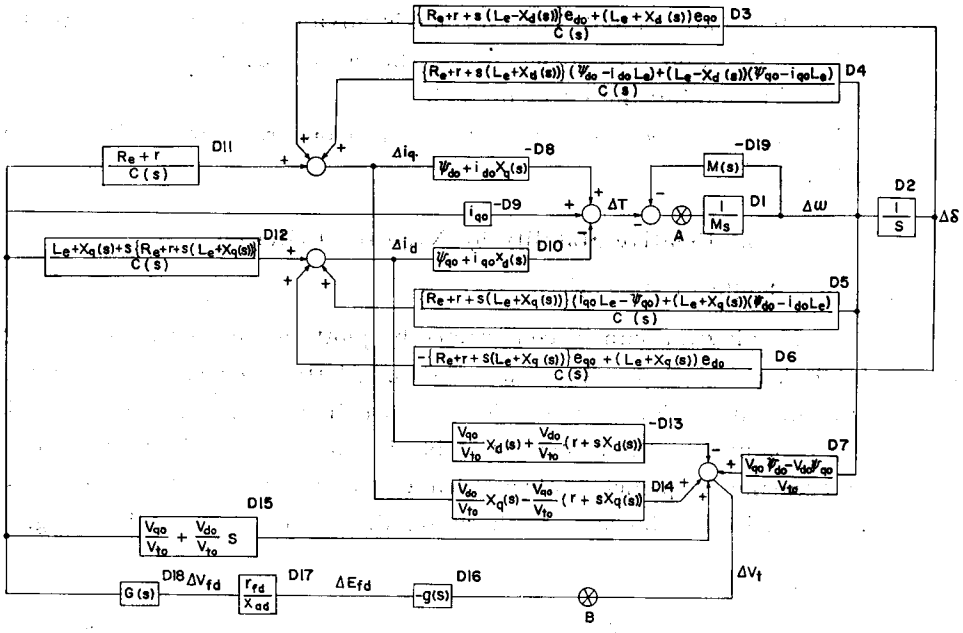

Fig. 6. Block diagram of the synchronous machine connected to infinite receiving bus.

controls. The dynamic stability of the set of equations described above depends upon the coefficients of the various terms which are dependent upon the machine loading as well as upon the characteristics of the controls.

To apply the Nyquist method to the above block diagram, it is cut at some point and the frequency response of the open loop transfer function is calculated. In Fig. 6 the point A is selected for the cut point for the reason that the basic stability phenomena include electro-mechanical oscillations and their damping, or the point B, for the reason that dynamic stability is greatly affected by AVR. In the case of the cut point being A, Fig. 6 results in Fig. 7, where the change of the input-torque into the alternator and the change of the angular velocity of the rotor are assumed to be the input signal and the output signal, respectively. Point B being selected, Fig. 8 is obtained, where the input is the change of the excitation voltage and the output is the

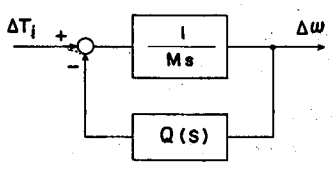

Fig. 7. Block diagram for torque-feedback.

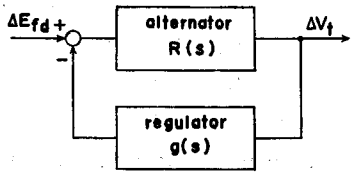

Fig. 8. Block diagram for voltage-feedback.

change of the terminal voltage. The former is advantageous in analyzing the mechanical equation and the movement of the governor, and the latter is profitable for determining the effect of AVR.

Mason's rule[4] is used to obtain the open loop transfer function (see Appendix D).

3. Relative Stability by Nyquist's Criterion

3-1 Nyquist's Sability Criterion

The Nyquist diagram can be constructed by plotting the open-loop transfer function of Fig. 6 for $s=j\omega$ over a range of ω. Plotting for values of s from 0 to $+j\infty$ results in a digram of the form shown in Fig. 9. Although that is a simplified explanation, the system is stable if its Nyquist diagram, traced out with increasing frequencies, always leaves the critical point $-1+j0$ at its left (Fig. 9 (a)); if the diagram is otherwise, the system is unstable (Fig. 9 [b]).

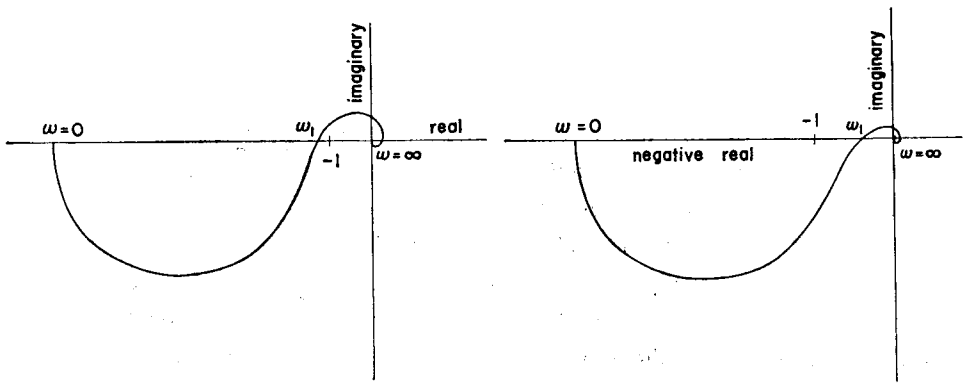

a) Stable b) Unstable

Fig. 9. Typical Nyquist plots.

3-2 Relative Stability by Nyquist's Criterion

Once it has been shown by application of the Nyquist criterion that the system is stable, the next point of interest in an analysis is the problem of transient performance. Even though a system may be absolutely stable, it is certainly possible that the system may be greatly underdamped and have an excessive overshoot or too long a duration of oscillation to be acceptable practically.[5] Thus, a knowledge of the degree of stability is frequently more important than merely knowing whether, under certain operating conditions, the machine is stable or not. In this section, the concept of relative stability is developed applying the Nyquist criterion.

A profitable approach to the evaluation of relative stability consists of investigating different paths from a conventional Nyquist's criterion in the s-plane[4]. In Fig. 10 s is changed from $-\sigma-j\infty$ to $-\sigma+j\infty$ along a line σ units to the left of the $j\omega$ axis, closing as usual in an infinite semicircle to the right. If no zeros of the characteristic equation are to the right of this line, the transient step response damps out at a rate greater than σ, that is, in any output terms of the form $Ae^{-\alpha t}\cos(\omega_n t+\phi)$, $\alpha>\sigma$.

Another path might be from the origin radially out along a line such that $s=\omega_n\varepsilon^{j\theta}=\omega_n(-\cos\psi+j\sin\psi)$ or $s=\omega_n(-\zeta+j\sqrt{1-\zeta^2})$, where $\zeta=\cos\psi$ is the damping factor ($\sigma=\zeta\omega_n$), thence clockwise around the usual infinite semicircle, back along a radial line with ponits conjugate to the first line, and into the origin (Fig. 11)[4,6]. Such a path would locate roots of the characteristic equation that give rise to specified damping factors.

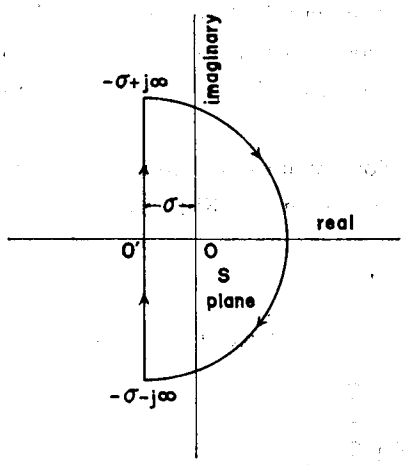

Fig. 10. Contour for Nyquist relative stability criterion (All oscillations have a damping ratio greater than σ).

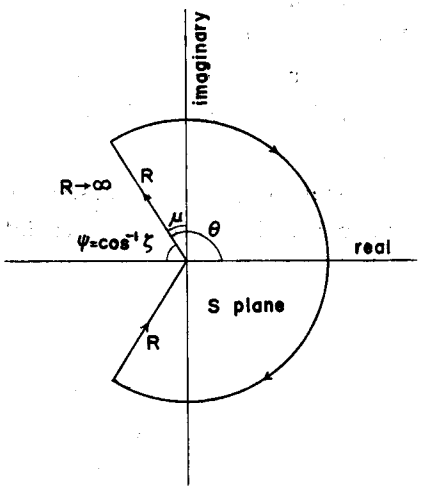

Fig. 11. Contour for Nyquist relative stability criterion (All oscillations have a damping factor greater than $\sin\mu$).

Table 1. List of the system constants.

T_a=0.2 sec.	K_f=40	L_e=0.6
T_e=1.0 sec.	K_e=1	R_e=0.06
T_s=1.0 sec.	K_s=0.8	V_t=1.1
T_g=0.8 sec.	K_g=0.8	
T_h=0.25 sec.	M=10 sec.	
r_{fd}=0.00107	r=0.002	r_{kd}=0.00318
r_{kq}=0.00318		
x_{ad}=1.86	x_{aq}=1.86	x_{fl}=0.14
x_{al}=0.14	x_{kql}=0.04	x_{kql}=0.04

Nyquist diagrams at the operating point of unit power and the unit power factor are shown in Fig. 12 where s is changed from $-\sigma+j0$ to $-\sigma+j\infty$. The value of σ was varied from 0.0 to 0.002 and shown as a parameter in the figure. As σ becomes large the phase lag becomes large and the system in this example is regarded as unstable when $\sigma=0.0015$. That is, an oscillation which decays to $1/\varepsilon$ of its initial amplitude at least in 1.77 sec. is involved in this operating point. Fig. 13 shows Nyquist diagrams at the same operating point when s is changed from 0 to $jRe^{j\mu}(R\to\infty)$. In this case the point of $\omega=0$ is immovable regardless of the value of μ but as μ grows greater, the phase lag becomes larger and the system is regarded as unstable when $\mu=20°$.

Fig. 14 shows the operating domain restricted by various values of σ. The curve is plotted by obtaining the critical value of power output changing the power factor angle, when the Nyquist diagram may be plotted only near the $(-1,0)$ point. Oscillations of long duration are found at the region of lagging power factor and a machine operating at about 0.5 per-unit power at a power factor angle of about $-15°$ is most stable from the viewpoint of the damping ratio.

An operating domain, restricted by various values of damping factor, is shown in Fig. 15. Trends of variation are the same as Fig. 14.

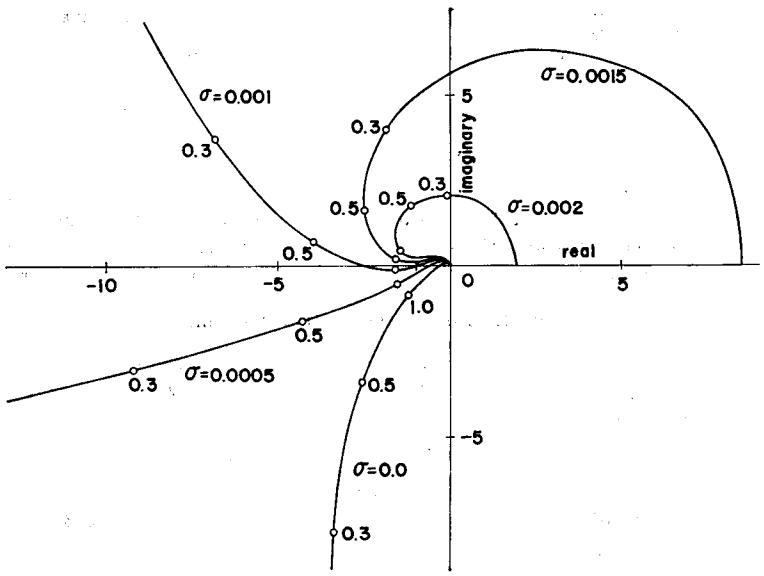

Fig. 12. Nyquist's loci for various values of σ (operating point: $|W|=1.0$ and $\phi=0°$).

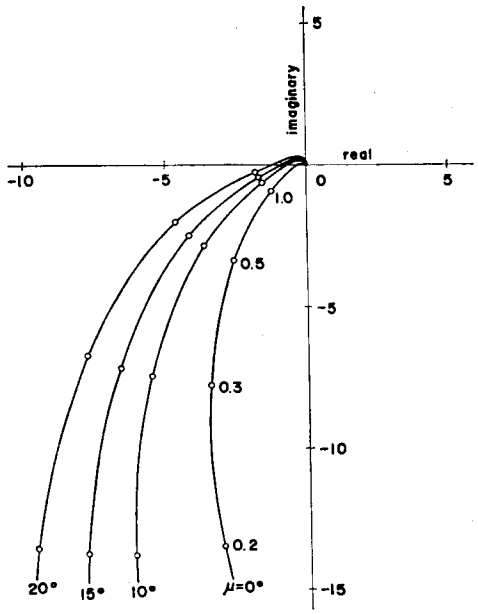

Fig. 13. Nyquist's loci for various values of μ (operating point: $|W|=1.0$ and $\phi=0°$).

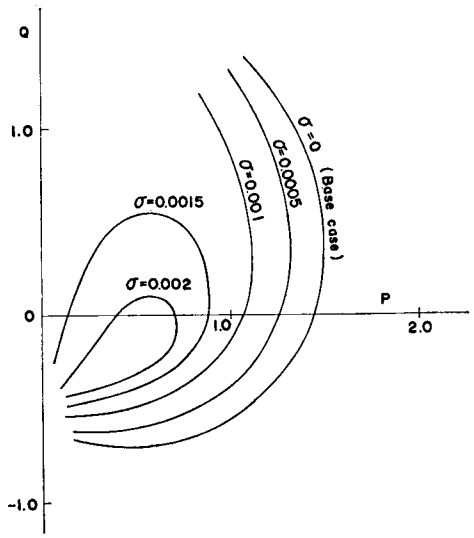

Fig. 14. Curves of constant relative stability (σ: damping ratio of oscillations).

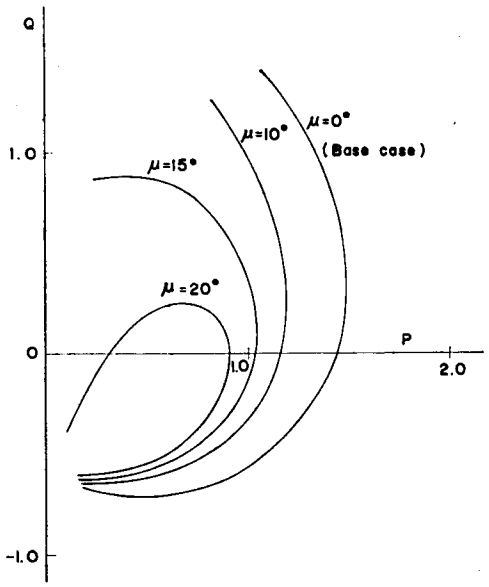

Fig. 15. Curves of constant relative stability ($\sin\mu$: damping factor of oscillations).

4. Indicial Response Analysis

The system is set up according to Fig. 6, which is in a linearized form, and transients resulting from a disturbance show how the system would respond if this disturbance were infinitesimally small. The equations representing the system can be assumed as linear only in the close neighborhood of the steady-state conditions for which the particular coefficients apply. Thus, for the response to actual finite disturbances a different representation of the machine would be required, but in general the block diagram given in section 2-5 can be used to provide approximate results for small finite variations. In this section the step signal response of the block diagram shown in Fig. 7 and Fig. 8 is calculated to investigate the structure of oscillations and the cause of instability.

If $W(s)$ and $V(s)$ are the closed-loop transfer functions of the block diagrams shown in Fig. 7 and Fig. 8, respectively, they are given by the following equations,

$$W(s)=\frac{1/Ms}{1+Q(s)/Ms} \tag{42}$$

$$V(s)=\frac{R(s)}{1+g(s)\cdot R(s)} \tag{43}$$

If $v(t)$ is the indicial response of $V(s)$, $v(t)$ represents the response of the terminal voltage v_t according to the step-change of the excitation voltage E_{fd}. Similarly $w(t)$ is defined to represent the response of the angular velocity ω to the step-change of the input torque T_M.

$v(t)$ and $w(t)$ may be calculated by considering a low-frequency square wave with unity magnitude shown in Fig. 16 applied to the system[7]. Expressed as a Fourier series, the square wave signal is,

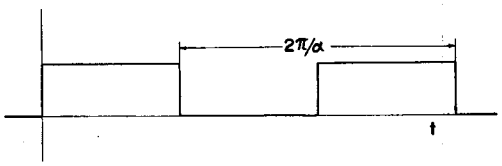

Fig. 16. Low-frequency square wave (for the calculation of indicial response).

$$\frac{1}{2}+\frac{2}{\pi}\sum_{n=0}^{\infty}\frac{\sin(2n+1)\alpha t}{2n+1} \tag{44}$$

If the period $2\pi/\alpha$ is sufficiently long, a steady-state condition is established before the end of the half cycle. The response of the system to the square wave in the case of Fig. 7 is

$$W(t)=\frac{G_0}{2}+\frac{2}{\pi}\sum_{n=0}^{\infty}\frac{G_{2n+1}}{2n+1}\sin\{(2n+1)\alpha t+\varphi_{2n+1}\} \tag{45}$$

Where $G_n=|V(jn\alpha)|$ and $\varphi_n=argV(jn\alpha)$.

In the practical computation, the duration of the positive half of the square wave is 20π sec., and terms up to those corresponding to 20 rad. (3.18 Hz) are included.

Fig. 17 (a), (b), (c), and (d) show the variation of $v(t)$ with time for various values of $|W|$ (absolute value of apparent power) as the machine operates at the unit power factor. From these figures, it was deduced that the damping of the oscillation is the fastest when $|W|=0.5$; as the value of $|W|$ gets large, the frequency of oscillation becomes low, although it becomes rather high near the stability limit, the mean value of which is about 0.25 Hz. This oscillation is considered to be caused by the combination of machine and

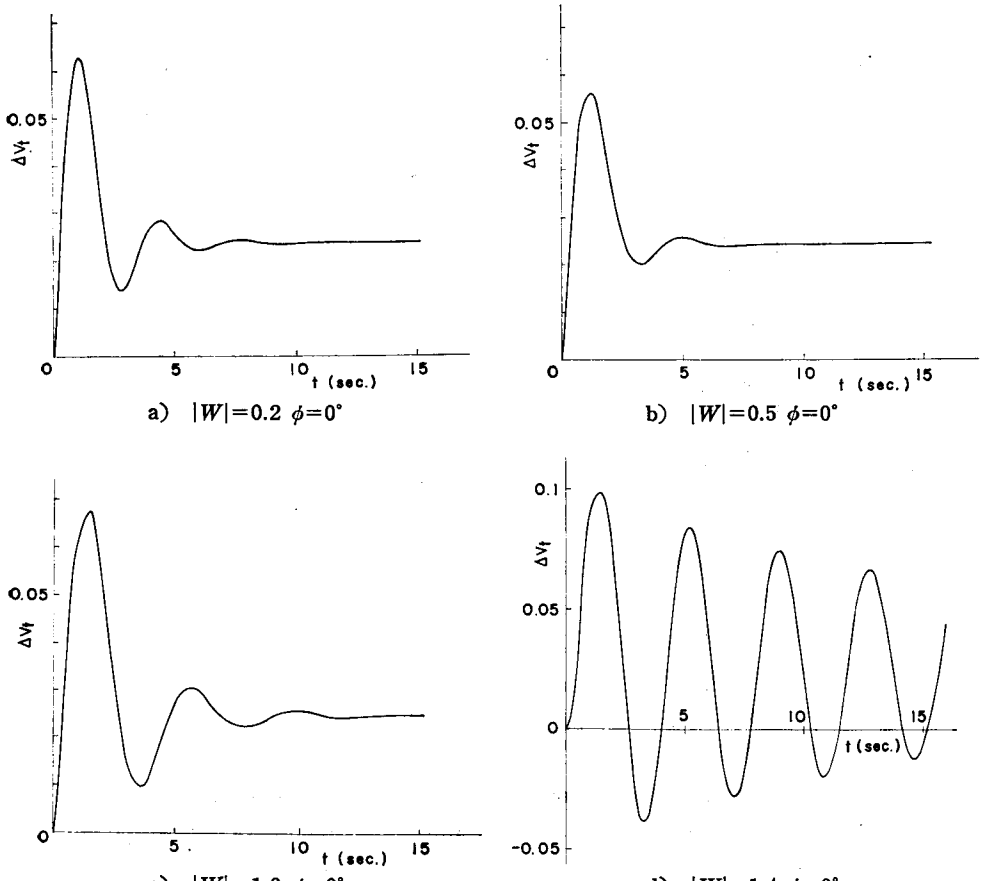

a) $|W|=0.2$ $\phi=0°$ b) $|W|=0.5$ $\phi=0°$

c) $|W|=1.0$ $\phi=0°$ d) $|W|=1.4$ $\phi=0°$

Fig. 17. Step signal response of terminal voltage.

regulator characteristics.

$w(t)$ for various values of $|W|$ are shown in Fig. 18 (a), (b), and (c) as the machine operates at the unit power factor. When the value of $|W|$ is small, only oscillation of high frequency appears and when the value of $|W|$ approaches the stability limit, an oscillation of low frequency appears as shown in Fig. 17. Instability occurs at this frequency. An oscillation of high frequency, whose mean value is about 1.1 Hz, was considered to be due to the interference between the mechanical and electrical torque.

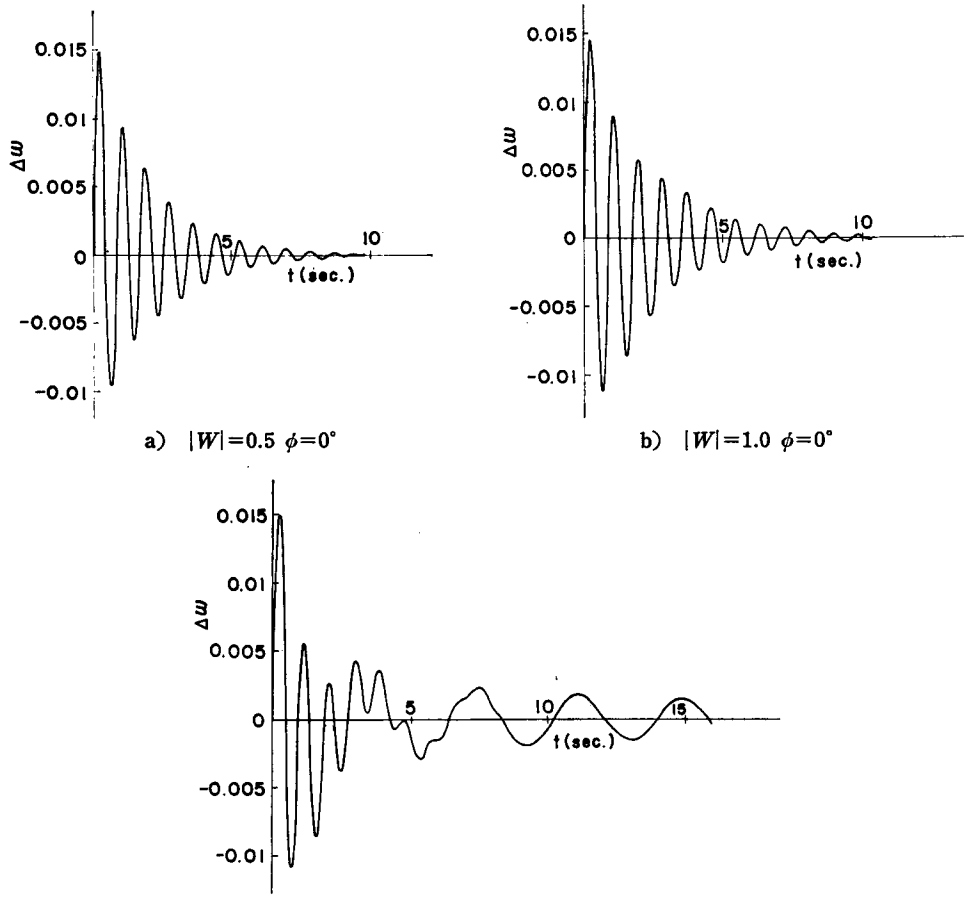

Fig. 18. Step signal response of angular velocity.

Fig. 19 (a), (b), and (c) shows the indicial response $w(t)$ for various values of the inertia constant when the machine operates at unit power and the unit power factor. It can be seen from these figures that the frequency is almost inversely proportional to the square root of the value of the inertia

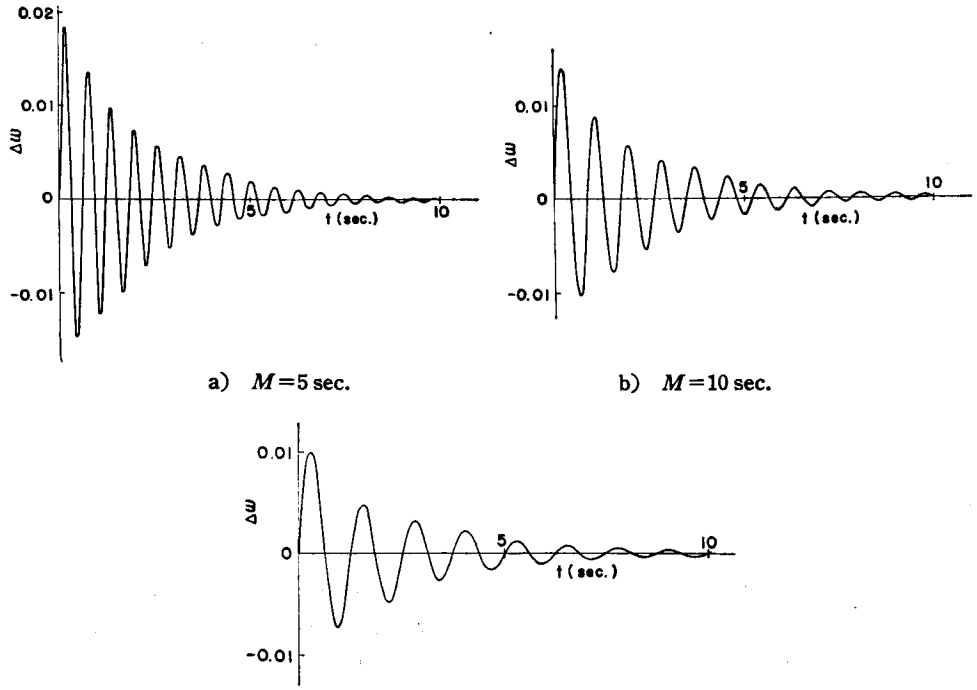

a) $M=5$ sec. b) $M=10$ sec.

c) $M=20$ sec.

Fig. 19. Step signal response of angular velocity (operating point: $|W|=1.0$ and $\phi=0°$).

constant. It was ascertained from the above consideration that the oscillation of high frequency involved in $w(t)$ is due to the interference between the mechanical and electrical torque.

The above consideration holds true for various power factor angles. Consequently, it can be said that the dynamic stability phenomenon is mainly governed by the feedback loop of the voltage regulator.

5. Measure of Relative Stability

Hitherto, most studies on power system stability have been restricted mainly to the problem of whether the system can be operated stably or not after some kind of disturbance, i. e., the problem of stability criterion; little attention has been paid to quantification of the degree of stability. On the other hand, some kind of performance index is required to effect optimum control of the electric power system. In this section a measure of dynamic stability is defined on the basis of the results obtained in the foregoing section and the degree of stability is investigated by this measure.

Since it was found from the results of the foregoing section that the small

signal stability is mainly governed by the feedback loop of the voltage regulator and that the frequency of unstable oscillation approximately equals that of the oscillation of the terminal voltage, it is adequate to define a measure on the basis of the response of the terminal voltage to the step change of excitation voltage.

The integral squared error of the step response of the terminal voltage is defined as the measure of dynamic stability. The value of the measure is given as:

$$M_s=\int_0^\infty\left\{1-\frac{v(t)}{V(0)}\right\}^2dt \tag{46}$$

where M_s: integral squared error

$V(0)$: steady-state value of $v(t)$

This integral squared error has a definite value when the system is stable. It is evident from the definition of the measure that the smaller the value of the measure, the better will be the small signal performance of the system. Observation of trends in the variation of the measure as the system parameters are changed yields useful information within those parameter ranges that give stable operation. M_s in eqn. (46) can be calculated from the indicial response obtained in the foregoing section by means of numerical integration. The upper limit of the time in the integral does not need to be infinite since

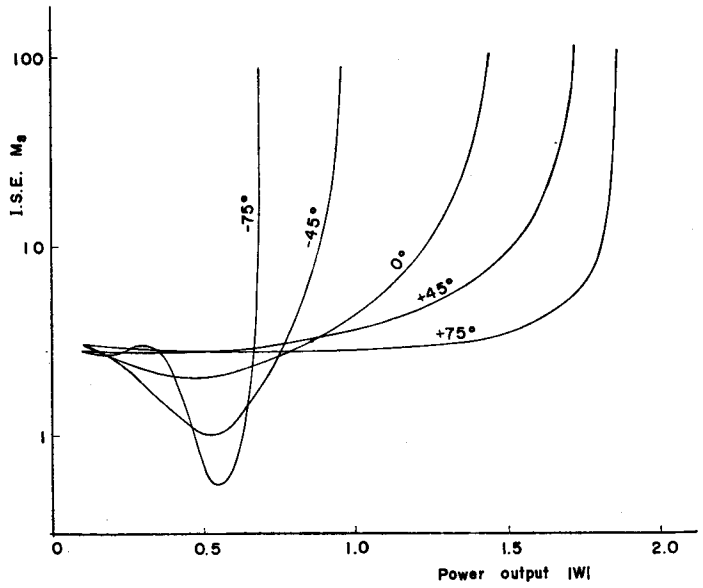

Fig. 20. Integral squared error vs. power output
(power factor angle: parameter)

the system is stable.

Fig. 20 shows the variation of the integral squared error M_s for various power factor angles as the power output is varied. The stability of the system decreases as the power output approaches a critical value, and M_s takes its minimum value when $|W|=0.5$.

From Fig. 20, equi-index curves may be drawn on a P-Q plane as shown in Fig. 21. The operations on one of these curves give the same integral squared error of the terminal voltage.

Fig. 22 shows the variation of the measure as the AVR gain K_f is varied. When the machine operates at 1.4 power (p. u.) at the unit power factor, the value of M_s increases rapidly both as the value of K_f decreases and as it increases, and the optimum value of K_f for this operating point is about four. On the other hand, when the machine operates at 1.0 power (p. u.) the system is stable without a voltage regulator.

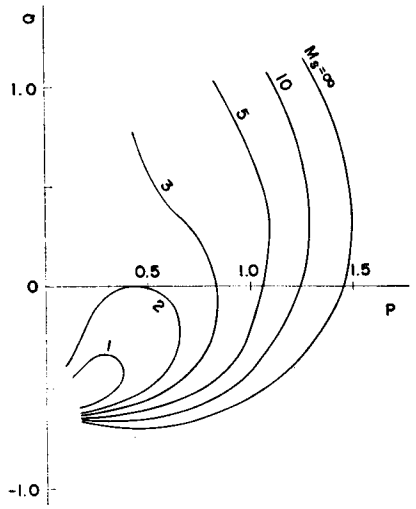

Fig. 21. Domain of operation restricted by various values of integral squared error.

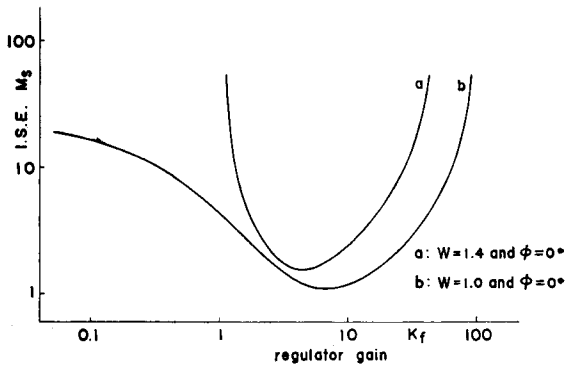

Fig. 22. Integral squared error vs. regulator gain.

6. Conclusions

The small signal performance of a single machine connected to an infinite bus through an external impedance has been represented in block diagram form, which illustrates the closed loop structure of the system equations, including the description of prime-mover power and excitation controls. The transfer function approach has one particular advantage in that each component can be treated separately and the effect of each on stability can be

obtained directly. Two kinds of open-loop transfer functions, related to voltage feedback and torque feedback, have been calculated via Mason's rule and the small perturbation stability characteristics have been studied by means of frequency response analysis and indicial response analysis based on frequency response. These methods, in contrast with others, avoid the need to solve for the roots of the characteristic equation. Through these analyses, it has been found that the small signal performance of the system is governed mainly by the loop of the alternator and the voltage regulator. According to this fact, the integral squared error of the terminal voltage responding to the step change of excitation voltage has been proposed as the measure of relative stability. The effects of the regulator gain have been investigated using this measure.

The results of the analyses are as follows:

1) In the overexcited region, poorly damped oscillations may be encountered at load levels considerably lower than the absolute stability limit. On the other hand, in the underexcited region, the operating state may approach the stability limit rather quickly with changing load.

2) From the results of the investigation using the measure of relative stability, it has been shown that there exists an optimum value for the voltage regulator gain.

Acknowledgement

The authors wish to thank Prof. C. Uenosono for his helpful comments and discussion. They also wish to thank Mr. S. Ihara for his suggestion which motivated this study.

List of Symbols

ψ_d, ψ_q = direct and quadrature axis armature flux linkages
ψ_{kd}, ψ_{kq} = direct and quadrature axis amortisseur flux linkages
ψ_{fd} = field flux linkage
e_b, e_d, e_q = infinite bus voltage and its direct and quadrature components
v_t, i_t = machine terminal voltage and current
v_d, v_q, i_d, i_q = direct and quadrature axis voltages and currents
i_{kd}, i_{kq} = direct and quadrature axis amortisseur currents
v_{fd}, i_{fd} = field circuit voltage and current
$E_{fd}=v_{fd}x_{ad}/r_{fd}$ = air-gap line, open-circuit excitation voltage
x_{ffd}, x_{kkd}, x_{kkq} = rotor-circuit self-reactances on d- and q-axis

x_{ad}, x_{aq}=mutual reactances on d- and q-axis
x_{al}=armature leakage reactance
x_{fl}=field leakage reactance
x_{kdl}, x_{kql}=leakage reactances of d- and q-axis amortisseur circuits
r_{fd}, r_{kd}, r_{kq}=rotor-circuit resistances on d- and q-axis
r=armature resistance
ω_0=rated angular frequency, rad./sec.
ω=instantaneous angular frequency, rad./sec.
$G(s)$=operational transfer function between v_{fd} and ψ_d
$X_d(s)$, $X_q(s)$=generator inductances in operational form
Z_e, R_e, L_e=eqiuvalent system impedance, resistance and reactance
δ=angle between q-axis of machine and its terminal voltage, rad.
T_M=torque input to rotor
T=air-gap torque
M=inertia constant, sec.
$g(s)$=transfer function of voltage regulator
K_f, K_e, K_s, T_e, T_a, T_s=voltage regulator constants
$M(s)$=transfer function of governor
K_g, T_g, T_h=governor constants

References

1) Shackshaft, G.: "General-purpose turbo alternator model", *Proc. IEE*, Vol. 110, No. 4, April 1963.
2) Prabhashankar, K,. and Janischewsyj, Wasyl: "Digital simulation of multimachine power systems for stability studies", *IEEE, Trans. Power Apparatus and Systems*, Vol. PAS-87, No. 1, January 1968.
3) Ewart, D. N., and DeMello, F. P.: "A digital computer program for the automatic determination of dynamic stability limits", *IEEE, Trans. Power Apparatus and Systems*, Vol. PAS-86, No. 7, July 1967.
4) Watkins, B. O.: *Introduction to Control Systems*, McGraw-Hill, New York, 1962.
5) Thaler, G. J., and Brown, R. G.: *Servomechanism Analysis*, McGraw-Hill, New York, 1953.
6) Stojić, M. R., and Šiljak, D. D.: "Generalization of Hurwitz, Nyquist and Mikhailov stability criteria", *IEEE Trans. on Automatic Control*, July 1965.
7) Jacovides, L. J., and Adkins, S.: "Effect of excitation regulation on synchronous-machine stability", *Proc. IEE*, Vol. 113, No. 6, June 1966.

Bibliography

1) Hayashi, M., Ihara, S., and Ohsawa, Y.: "A measure of dynamic stability of one-machine system", *JIEEI*, Vol. 90, No. 11, 1970.
2) Messerle, H. K., and Bruck, R. W.: "Steady-state stability of synchronous generators

as affected by regulators and governors", *IEE*, No. 134 S, June 1955.
3) Aldred, A. S., and Shackshaft, G.: "A frequency-response method for the predetermination of synchronous-machine stability", *IEE*, No. 393 S, July 1960.
4) Smith, O. J. M.: *Feedback Control Systems*, McGraw-Hill, New York, 1958.
5) DeMello, F. P., and Concordia, C.: "Concepts of synchronous machine stability as affected by excitation control", *IEEE, Trans. Power Apparatus and Systems*, Vol. PAS-88, No. 4, April 1969.

Appendix A Park's Axis Transformation

Park's transformation may be written as:

$$\boldsymbol{w}_d = P(\theta)\boldsymbol{w}_a \tag{A-1}$$

$$P(\theta) = \frac{2}{3}\begin{Bmatrix} \cos\theta & \cos\left(\theta-\frac{2}{3}\pi\right) & \cos\left(\theta+\frac{2}{3}\pi\right) \\ -\sin\theta & -\sin\left(\theta-\frac{2}{3}\pi\right) & -\sin\left(\theta+\frac{2}{3}\pi\right) \\ 1/2 & 1/2 & 1/2 \end{Bmatrix} \tag{A-2}$$

where $\boldsymbol{w}_d$ is the column vector of Park's quantities and $\boldsymbol{w}_a$ is that of phase quantities.

Appendix B Machine Equations

Direct-axis flux linkage

$$\psi_{fd} = x_{ffd}\cdot i_{fd} - x_{ad}\cdot i_d + x_{fkd}\cdot i_{kd} \tag{B-1}$$

$$\psi_d = x_{ad}\cdot i_{fd} - x_d\cdot i_d + x_{ad}\cdot i_{kd} \tag{B-2}$$

$$\psi_{kd} = x_{fkd}\cdot i_{fd} - x_{ad}\cdot i_d + x_{kkd}\cdot i_{kd} \tag{B-3}$$

Quadrature-axis flux linkage

$$\psi_q = -x_q\cdot i_q + x_{aq}\cdot i_{kq} \tag{B-4}$$

$$\psi_{kq} = -x_{aq}\cdot i_q + x_{kkq}\cdot i_{kq} \tag{B-5}$$

Direct-axis voltage

$$v_{fd} = s\psi_{fd} + r_{fd}\cdot i_{fd} \tag{B-6}$$

$$v_d = s\psi_d - r\cdot i_d - \omega\cdot\psi_q \tag{B-7}$$

$$0 = s\psi_{kd} + r_{kd}\cdot i_{kd} \tag{B-8}$$

Quadrature-axis voltage

$$v_q = s\psi_q - r\cdot i_q + \omega\cdot\psi_d \tag{B-9}$$

$$0 = s\psi_{kq} + r_{kq}\cdot i_{kq} \tag{B-10}$$

Appendix C Derivation of Transfer Function

Eliminating $\Delta\psi_d$, $\Delta\psi_q$, Δv_d, and Δv_q from eqns. (20)-(23) and (29), Δv_t is

given as follows:

$$\Delta v_t=\frac{v_{q0}\psi_{d0}-v_{d0}\psi_{q0}}{v_{t0}}\Delta\omega+\left\{\frac{v_{d0}}{v_{t0}}X_q(s)-\frac{v_{q0}}{v_{t0}}(r+sX_q(s))\right\}\Delta i_q-\left\{\frac{v_{q0}}{v_{t0}}X_d(s)+\frac{v_{d0}}{v_{t0}}(r+sX_d(s))\right\}\Delta i_d+\left\{\frac{v_{q0}}{v_{t0}}G(s)+\frac{v_{d0}}{v_{t0}}G(s)\cdot s\right\}\Delta v_{fd} \tag{C-1}$$

Eliminating $\Delta\psi_d$ and $\Delta\psi_q$ from eqns. (20), (21), and (29) to give:

$$\Delta T=\{\psi_{d0}+i_{d0}X_q(s)\}\Delta i_d-\{\psi_{q0}+i_{q0}X_d(s)\}\Delta i_d+i_{q0}G(s)\Delta v_{fd} \tag{C-2}$$

Eliminating Δe_d and Δe_q from eqns. (24)-(26), and substituting eqns. (20) and (21) into the resultant equations,

$$\{R_e+r+(L_e+sX_d(s))\}\Delta i_d-(L_e+X_q(s))\Delta i_q=sG(s)\Delta v_{fd}-(\psi_{q0}-i_{q0}L_e)\Delta\omega-e_{q0}\Delta\delta \tag{C-3}$$

$$(L_e+X_d(s))\Delta i_d+\{R_e+r+s(L_e+X_q(s))\}\Delta i_q=G(s)\Delta v_{fd}+(\psi_{d0}-i_{d0}L_e)\Delta\omega+e_{d0}\Delta\delta \tag{C-4}$$

Solving eqns. (C-3) and (C-4) for Δi_d and Δi_q,

$$\Delta i_d=A_1\Delta v_{fd}+A_2\Delta\omega+A_3\Delta\delta \tag{C-5}$$

$$\Delta i_q=B_1\Delta v_{fd}+B_2\Delta\omega+B_3\Delta\delta \tag{C-6}$$

where

$$A_1=\frac{\{R_e+r+(L_e+X_q(s))s\}sG(s)+(L_e+X_q(s))G(s)}{C(s)} \tag{C-7}$$

$$A_2=\frac{\{R_e+r+(L_e+X_q(s))s\}(i_{q0}L_e-\psi_{q0})+(L_e+X_q(s))(\psi_{d0}-i_{d0}L_e)}{C(s)} \tag{C-8}$$

$$A_3=\frac{-\{R_e+r+(L_e+X_q(s))s\}e_{q0}+(L_e+X_q(s))e_{d0}}{C(s)} \tag{C-9}$$

$$B_1=\frac{(R_e+r)G(s)}{C(s)} \tag{C-10}$$

$$B_2=\frac{\{R_e+r+(L_e+X_d(s))s\}(\psi_{d0}-i_{d0}L_e)+(L_e+X_d(s))(\psi_{q0}-i_{q0}L_e)}{C(s)} \tag{C-11}$$

$$B_2=\frac{\{R_e+r+(L_e+X_d(s))s\}e_{d0}+(L_e+X_d(s))e_{q0}}{C(s)} \tag{C-12}$$

$$C(s)=\{R_e+r+(L_e+X_d(s))s\}\{R_e+r+(L_e+X_q(s))s\}+(L_e+X_q(s))(L_e+X_d(s)) \tag{C-13}$$

Fig. 6 can be obtained from eqns. (31)-(34), (C-1), (C-2), and (C-5)-(C-13).

Appendix D Mason's Rule

Assume input node i and output node j, and let

Δ=the graph determinant

P_k=the kth forward path between i and j

Δ_k=the path factor or graph determinant Δ when all loops touching the kth path are deleted

Then Mason's rule is

$$T_{ij}=\frac{\sum_{k=1}^{n} P_k\Delta_k}{\Delta} \tag{D-1}$$

where T_{ij} is the input-output relation between nodes i and j, n is the total number of forward paths, and

Δ=1−(Σ all different loops)
+(Σ all different products of pairs of non-touching loops)
−(Σ all differennt products of triplets of non-touching loops)
+.....